University of Exeter coursework header sheet

ECMM102 Group Project (Meng) (A, TRM1+2 2015/6)

029228

1019571

620036449

Coursework: I2

Submission Deadline: Thu 28th Apr 2016 12:00

Personal tutor: Dr Prakash Kripakaran

Marker name: G Tabor

Word count: 11212

By submitting coursework you declare that you understand and consent to the University policies regarding plagiarism and mitigation (these can be seen online at www.exeter.ac.uk/plagiarism, and www.exeter.ac.uk/mitigation respectively), and that you have read your school's rules for submission of written coursework, for example rules on maximum and minimum number of words. Indicative/first marks are provisional only.

I2 Report

Wind Farm Layout Optimisation Using Genetic Algorithm

Guoxuan Liu

2015

4th year MEng Group Project

I certify that all material in this thesis that is not my own work has been identified and that no material has been included for which a degree has previously been conferred on me.

Signed..... .....

College of Engineering, Mathematics, and Physical Sciences
University of Exeter

I2 Report

ECMM102

Title:

Word count: 11212

Number of pages: 40

Date of submission: Wednesday, 27 April 2016

Student Name: Guoxuan Liu

Programme: MEng Electronic Engineering

Student number: 6200 36449

Candidate number: 029228

Supervisor: Professor Gavin Tabor

Abstract

As the energy market becomes more competitive and many current methods over estimate the total farm power output, new methods of wind farm optimisation are investigated. This report investigates the use of multi-objective genetic algorithm to optimise wind farm layout.

The projects aims to develop a modifiable multi-objective genetic algorithm, to maximise wind farm power output, minimise capital and operation & maintenance cost. The objectives are implemented in separate functions, to allow easy further improvement. The power objective modelled is the Jenson-Kasic wake model coupled with square summing method. The capital cost objective is modelled by considering the cost of survey, turbine, substation and cable cost. The operation & maintenance cost considers the cost of general office cost and individual turbine maintenance cost.

The individual tests of the objective functions have shown that the functions are implemented accurately. The test of the overall algorithm on small farms has shown the algorithm to determine expected optimal layouts. The test of the overall algorithm on large farm has shown an exponential relationship between power production and costs for optimal layouts.

As well as genetic algorithm implementation, computation cost reduction methods are investigated. Generalised Pareto-based scale-independent fitness function and crowding distance are both implemented and tested. The results have shown that the two have been correctly implemented, and is effective at reducing computation cost, by reducing the number of optimal samples stored in the archive throughout simulations.

Keywords: Genetic algorithm (GA), Multi-objective genetic algorithm (MOGA), Improved vector evaluated genetic algorithm (IVEGA), Generalised Pareto-based scale-independent fitness function (gp-siff), Relative distance behind rotor.

Table of contents

1. Introduction and background

The wind energy market is rapidly expanding; the total wind capacity worldwide has seen over a 17% cumulative growth in both 2014 and 2015 *(GWEC, 2016)*. With the crude oil price dropping by 60% in the past 5 years *(NASDAQ.com, 2016)*, coupled with the cuts in renewable subsidy in the UK *(Timperley, 2015)*, it is more important than ever to find new methods to reduce the cost of energy (COE) for the wind energy market to remain competitive.

$$COE = \frac{ICC*FCR+LRC}{AEP_{NET}} + O\&M \{1\}$$

Equation 1 shows how the COE can be calculated *(Walford, 2006)*. It uses the initial capital cost (ICC), fixed charge rate (FCR), levelised replacement cost (LRC), operation and maintenance (O&M) cost and the net annual energy production (AEP_{NET}).

$$AEP_{NET} = AEP_{GROSS} * Availability * (1 - Loss) \{2\}$$

Equation 2 shows how the AEP_{NET} can be calculated. This is affected by the operational hours (Availability) and other factors that reduce the expected energy production of a turbine (Loss). By maximising the turbine availability and minimising the energy loss, the AEP_{NET} can be maximised and thus reducing the cost of energy.

One major loss in large wind farm is due to wake effect. This is where upstream turbines reduce the wind speed for downstream turbines. Optimising the wind farm layout using wake models can help to mitigate this.

Genetic algorithms (GAs) are often used to optimise the wind farm layout *(Kusiak and Song, 2009), (Ituarte-Villarreal and Espiritu, 2011), (Wang, Liu and Zeng, 2009)*. This method can be extended to not only determine the optimal wind farm layout for power production, but to find the Pareto front between power production, initial capital cost and operation & maintenance (O&M) cost. This would determine the relationship between costs and energy production and give potential developers a series of optimal layouts to choose from.

The aim of this project is to develop a multi-objective GA (MOGA) that analyses the layouts of results on the Pareto front and determines the relationship between the three objectives. The objective models are from the evaluation or development work carried out by other members within the large project team. The algorithm is developed through evaluating various MOGA techniques, adapting different methods to optimise layouts and present the Pareto front. The project will also investigate methods of lowering computation cost.

2. Literature review

Literatures are reviewed in three sections. The first discusses several researches that have used GAs to determine the optimal wind farm layout to maximise farm power output. The second presents the sources of cost estimations. The final section compares several MOGAs, and determines the most suitable algorithm for wind farm layout optimisation.

2.1. Power output optimisation

The use of GAs in wind farm layout optimisation is addressed in literatures *(Kusiak and Song, 2009), (Ituarte-Villarreal and Espiritu, 2011), (Wang, Liu and Zeng, 2009)*. All literatures reviewed have used a binary 0-1 method to represent the absence or presence of wind turbines respectively, this representation method allows for easy analysis of optimised layout.

Ituarte-Villarreal et al. *(Ituarte-Villarreal and Espiritu, 2011)* models square and flat wind farm conditions. Unidirectional uniform winds are used through all simulations; meaning incoming wind angle and velocity are constant. Turbine numbers are also constant and turbines are separated into square sections. The consistency in farm size and turbine number eliminates cost variations. Lending the problem to a single objective problem, where one optimal solution can be determined by finding the layout with the highest power output.

Wang et al. *(Wang, Liu and Zeng, 2009)* analyses the effects of different gridding methods, including square, triangular and circular gridding, different wind direction and different grid densities. The algorithms goal is similar to research by Ituarte-Villarreal et al.. The problem is modelled as a single objective one, by keeping the turbine number constant in each scenario. The results have shown that the wind direction can have varying effects on the total farm efficiency depending on the gridding method, The conclusion is that the square gridding can produce satisfactory results for a single wind direction or a single dominant wind direction. Furthermore, the simplicity of square gridding method makes it the cheapest in terms of computational cost. The result on grid density has shown that higher density would produce a superior result; but the computational cost needs to be considered. As the relationship between farm density and result quality is an inversely exponential one; the rate of change in economic efficiency slows as farm density increase.

Kusiak et al. *(Kusiak and Song, 2009)* have modelled the problem to be a bi-objective one. The primary objective is the power output of the farm; similar to Ituarte-Villarreal et al. and Wang

et al. but the secondary objective is the distance between turbines. The algorithm aims to reduce the distance between turbines to 4 rotor diameters. The power objective uses multidirectional non-uniform wind. Wind data is used as an input, the wind is split into 24 directional bins around a full circle so that each bin covers 15°; the velocity within each angle range is represented by nominal wind and its Weibull distribution. The use of multidirectional non-uniform wind ensures the yaw angle and wind fluctuation is accurately modelled. A dynamic power fitness function can be designed to include the capability of analysing the power production of multidirectional non-uniform wind. The optimised farm layouts are more realistic representations of real farms.

Kusiak et al. also used a power function to represent the true power-velocity relationship on the turbine. The power rating of the turbine modelled is split into 4 sections. 0W when the wind velocity is below the cut-in velocity; a linear power velocity relationship between cut-in and optimal wind velocity; an optimal power output level between optimal wind velocity and cut-out velocity; and back to 0W when wind velocity is higher than cut-out wind velocity, to ensure turbine safety. However, a general power function can be applied, when the power-velocity relation for wind turbines are not known.

$$P = \frac{1}{2} * \rho * A * V^3 * C_P \{3\}$$

Equation 3 *(npower, 2016)* above shows how wind turbine power can be calculated; it uses velocity (V), air density (ρ), swipe area (A), and a power coefficient (C_P). The first three variables are used to calculate the fluid power. The final variable is the power coefficient; this has values between 0.35 and 0.45 for well-designed turbines *(npower, 2016)*. The power coefficient value used throughout the design will be 0.4.

Although Kusiak et al. have modelled the problem as a bi-objective one; the second objective of distances between turbines can be set as criteria rather than an objective, as a finite minimum value can be reached.

The three literatures reviewed above have shown how GAs can be used to optimise wind farm layouts with the primary objectives being to maximise the power output. The results are series of optimal layouts, differentiated by the farm condition and turbine number.

The above researches have shown that the use of square gridding method with medium grid density yields quality result with low computation cost. Although all research could benefit by extending the algorithm to MOGA, optimise layouts between power and cost.

2.2. Costs

The capital cost can be easily estimated, as the farm location and size are constants in each simulation, the majority of the capital cost can be assumed to be the same for all wind farms sampled. By reviewing data provided by the Crown Estate *(The Crown Estate, n.d.)*, a simple near linear relationship can be obtained for the cost of the farm as shown in equation 4.

$$Captial = BC + SC + TC + CC \ \{4\}$$

The capital cost is the sum of basic cost (BC), substation cost (SC), turbine cost (TC) and cable cost (CC). The basic cost is constant for all sampled farms, as the farm location and size are kept constant for each evaluation; these costs include development and consent as well as installation and commission. The substation cost is the product of individual substation costs and total number of substations, which can be found by rounding up the result of turbine numbers over substation coverage. The turbine cost is the product of total turbine number and individual turbine cost; the individual turbine cost includes the individual turbine foundations as well as the cost of nacelle, rotor and tower. Lastly, cable cost is the product of the minimum cable length and cable unit cost, the minimum cable length is found by using a Steiner Tree algorithm *(Tehranipoor, 2008)*. The algorithm finds the minimum cable length to connect all turbines a substation can cover.

$$O\&M = TL * OC + (TL - WT) * TOC * TN \ \{5\}$$

Equation 5 shows that the O&M cost can be calculated. It uses the turbine lifespan (TL), warranty time (OT), turbine operation cost (TOC), total turbine number (TN), and office cost (OC), which includes the basic annual costs to operate the wind farm. Turbine lifespan of 20 years is used in the algorithm, this is the estimated lifespan commonly used by the industry and Government for wind farm calculation *(Windmeasurementinternational.com, 2016)*. Although it is worth noting that studies have suggested the real life span of wind turbines to be shorter than expected *(Wind turbines' lifespan far shorter than believed, study suggests, 2016)*, *(Mendick, 2012)*. The office cost relates to the facility cost to operate and monitor the wind farm, data by Crown Estate *(The Crown Estate, n.d.)* estimate this to be around £5 million per annum for a 500MW farm. The warranty time is between 5 and 15 years *(Renewables First, 2016)*, depending on the turbine manufacturer, 5 years is used as a base in the program. Lastly, the turbine operation cost is the product of total turbine number and individual operation cost, which is estimated to be £102k per annual for large offshore turbines *(Renewables First, 2016)*.

Although all major contributors to the capital cost are easily found or can be easily estimated according to farm size and the number of turbines, the O&M cost information is more vague, with many papers *(The Crown Estate, n.d.), (Windmeasurementinternational.com, 2016), (Wind-energy-the-facts.org, 2016), (International Renewable Energy Agency, 2012)* suggesting it is around 10% to 30% of capital cost over turbine operating lifetime. The large range of value for O&M cost is due to the lack of attention paid to the area in the early years of wind farm development. But with the increase in large offshore wind farms in recent years *(Milborrow, 2010)*, investors are paying more attention to the O&M cost and developing models to both calculate the overall cost and to predict turbine breakdowns, in order to minimise turbine offline time. The O&M cost is likely to reduce over the coming years with the application of more accurate statistical modelling in O&M.

It is evident that the capital cost and O&M cost are both heavily dependent upon the turbine number; therefore it is possible to combine these two objectives into one, and create a bi-objective GA. In order to meet the brief of a three objective algorithm the two cost objectives are kept separate, to ease any future improvements that can be made if better statistical modelling of O&M costs are developed and tested.

2.3. Multi-objective genetic algorithm (MOGA)

In the research by Kumar et al. *(Kumar, Saxena and Kumar, 2014)*, where the concept of MOGA is discussed and several MOGAs are compared. The size of Pareto space covered are of the same level for all algorithms compared, the uniform distribution of results are all of similar levels for algorithms compared, with the exception of Strength Pareto Evaluation algorithm (SPEA). This performed better than the rest in terms of uniform distribution. Lastly, the comparison of computation effort between all algorithms have shown the Vector Evaluated GA (VEGA) and Murata & Ishibushi MOGA (MIMOGA) are superior to the rest. The computation effort is calculated by the number of objective functions evaluated over a fixed period of simulation time, indicating the VEGA and MIMOGA requires less simulation time.

Research by Murata & Ishibushi *(Murata and Ishibuchi, 1995)* on MIMOGA and research by Zhang & Fujimura *(Zhang and Fujimura, 2010)* on Improved VEGA (IVEGA) have shown that both low computational effort algorithms use a tentative elite population preservation method, which preserves non-dominated solutions, until a termination criterion is met.

The two algorithms differ in the selection process and elitist strategy. The MIMOGA uses a weighted sum approach when selecting samples to perform crossover and mutation operators. In comparison, the IVEGA uses a proportional selection also known as roulette wheel selection (RWS) to select samples to be operated on further. MIMOGA requires more calculation during the selection process, therefore would be more computationally costly.

The MIMOGA uses a more liberal approach in elitist strategy compared to IVEGA, when preserving non-dominated solutions. The MIMOGA fills the tentative elite file by randomly selecting non-dominated solutions, whereas IVEGA uses generalised Pareto-based scale-independent fitness function (gp-siff) coupled with individual crowding distance to reduce tentative elite string size when the number of non-dominated samples preserved exceeds the predefined elite string size. Although the IVEGA requires higher computational effort when preserving elite samples, the use of stricter elitist reduction method would be more beneficial for three objective GA, as the number of non-dominated samples could easily exceed number of samples required.

3. Theoretical background and design

Before a detailed algorithm is designed, a series of acceptable assumptions are made to ensure a realistic and accurate objective calculation.

The design of the algorithm is presented in the same order as the literature review. Sections 3.2 and 3.3 details how the power and cost objective function are designed. Section 3.4 shows how the algorithm is adapted and implemented.

The final section shows a series of experiments designed to emphasis the results of individual functions; all experiments are designed to allow easy result analysis.

3.1. Assumptions

3.1.1. Farm size and location

The farm size and location are assumed to be constant throughout each simulation. The wind farm is assumed to be offshore, as offshore farms have little surface roughness variation. The small surface roughness variation allows the assumption of levelled turbine height to be acceptable. The assumption that all samples in a simulation have the same farm size and location ensures that wind data remain constant for all layout samples evaluated. Constant

farm size and location also means that some factors that affect the costs, such as the water depth and distance from shore also remain constant.

3.1.2. Wind data

All turbines are assumed to be operating in the same height. The wind data is assumed to be the same across the farm. Research by Kusiak et al. *(Kusiak and Song, 2009)* has shown that 24 angle range bins can represent the wind, each with its own velocity distribution. The power function in this research is designed to include the ability to incorporate wind angle and velocity change.

3.1.3. Turbine type

The wind turbines modelled are considered homogenous; they have the same dimensions and the same power-velocity relationship. This is true for large wind farms as investors often use the same turbine supplier to reduce the O&M costs.

3.1.4. Turbine size

The turbine size are assumed to be 100m in diameter, this is the norm for large industrial wind turbines *(Aweo.org, 2016)*. The true turbine diameter only affects the swept area when calculating turbine power. All other distances used, such as the farm size and separation distance, are measured relative to the turbine diameter.

3.1.5. Turbine locations

The wind turbines are given individual Cartesian coordinates (x, y), which represent the location of turbines relative to the top left corner of the farm. The use of Cartesian coordinates reduces the farm into a 2D top view image, ignoring any changes in height.

3.1.6. Turbine separation distance

According to the Government Planning Portal *(Planningni.gov.uk, 2016)*, the turbine separation distance needs to be between 3-10 rotor diameters. In the layout study by Kusiak et al. *(Kusiak and Song, 2009)*, turbines are separated by at least 4 rotor diameters, to avoid hazardous loads. The study uses 4 rotor diameters as the optimal separation distance, making it the second objective. However, instead of specifying the separation distance in this paper, the separation distance is set as a variable that can be modified; the dynamic nature of the separation distance allows the algorithm to be used on a variety of site circumstances.

3.2. Power fitness evaluation

Wake effect is a major factor that reduces the wind turbine performance *(Renkema, 2007)*. Many studies and experiments have been conducted on this effect; it is accepted as a major contributor of sub-optimal farm performance. Therefore power fitness is evaluated using a wake effect model to determine the resultant velocity and power output of wind farm.

A research paper, by Douwe J. Renkema, on 'Validation of Wind Turbine Wake Models' *(Renkema, 2007)*, have compared several wake models and wake summing methods currently available. This is similar to the work carried out by another member of the project group, who has suggested the use of the Jenson-Katic model and the squares summing method for power fitness *(Withams, 2016)*. The wake model and summing methods are shown in equations 6 and 7 respectively *(Renkema, 2007)*.

$$1 - \frac{u}{U} = \frac{\left(1-\sqrt{1-C_t}\right)}{(1+2ks)^2} \{6\}$$

$$(1 - \frac{u_i}{U})^2 = \sum_j 1 - \frac{u_{ij}}{u_j} \{7\}$$

Equation 6 shows how the velocity deficit (1-u/U) caused by one turbine can be calculated. It uses wind velocity at the turbine (u), uninterrupted wind velocity (U), thrust coefficient (C_T), wake decay constant (k), and relative distance behind rotor (s), s = x/D, x is distance between turbines and D is the turbine diameter. The wake decay constant is generally taken as 0.075 for land cases and 0.04 for offshore cases *(Renkema, 2007)*.

Equation 7 shows how the deficit caused by multiple turbines can be summed. The summing method calculates wind speed at turbine i (u_i), using the uninterrupted wind speed (U), wind speed at turbine i due to the wake of turbine j (u_{ij}) and the wind velocity at turbine j (u_j). The summing method can be summarised, as the square of the total velocity deficit of a turbine, is equal to the sum of the square of velocity deficit caused by all other turbines.

Jenson-Katic wake model assumes linear wake spread; the wake diameter increases proportionally to the distance behind the turbine. Equation 8 shows how the wake diameter (D_w) can be calculated *(Renkema, 2007)*. It uses turbine diameter (D), wake decay coefficient (k) and relative distance behind rotor (s).

$$D_w = D \cdot (1 + 2ks) \{8\}$$

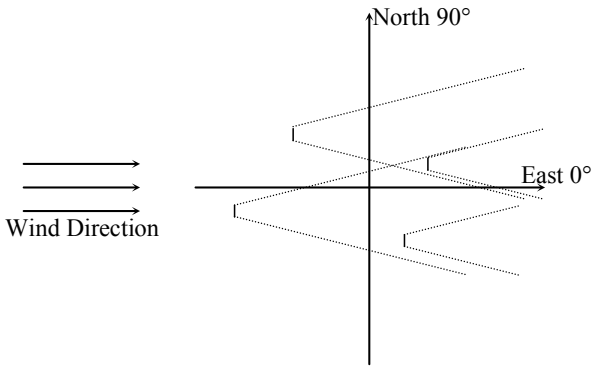

Figure 1 Illustration of turbine effect by the wake of other turbines

Figure 1 illustrates the linear spread of wake behind wind turbines. The four small vertical solid lines with dotted lines on either side represent wind turbines. The dotted lines represent the spread of wake corresponding to each turbine. The turbines are read as T1 to T4 from left to right, T1 and T2 and not covered by the wake of any turbine; therefore the speed at these turbines is the uninterrupted wind speed. The wind speed at T3 and T4 are lower than uninterrupted wind speed due to the wake effect from T1 and T2.

3.2.1. Angle correction

As the wind angle range considered is between 0° and 360°, which differs to the MATLAB calculation angle range of -90° to 90°, a correction is needed to rectify MATLAB calculated angles. Figure 3 shows the comparison between MATLAB calculated angles based on turbine distance, and the true angle between turbines. The difference is split into 4 quadrants, as the relationship between the calculated angle and true angle differ on either sides of the x-y-axis.

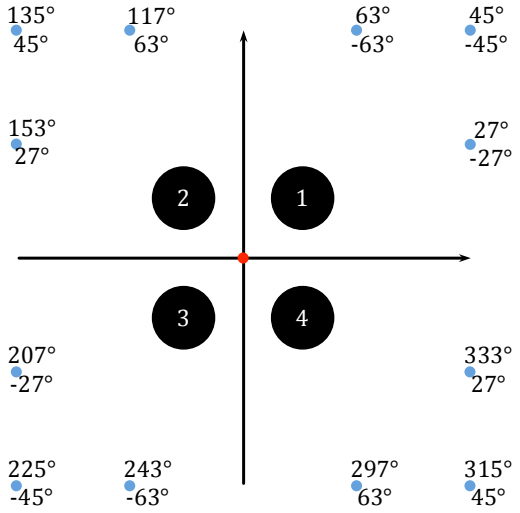

Figure 2 Comparison of MATLAB calculated angles to true angle

Figure 2 shows 12 turbines represent by blue dots that generate wake, which affects the turbine in the centre, represented by the red dot. Each affecting turbine has two corresponding angles, the top angle is the true angle, where east is 0° and north is 90°, between the affecting turbine and centre turbine, and the bottom angle is MATLAB calculated angle, using the Cartesian coordinates of the two turbines. The 12 sets of angles are separated into 4 quadrants, quadrant 1 includes angles from 0° to 90°, quadrant 2 includes 90° to 180°, quadrant 3 includes 180° to 270° and quadrant 4 includes 270° to 360°. The relationship between the true angle, θ_T, and MATLAB calculated angle, θ_C, within quadrants 1 to 4, are shown in equations 11 to 14 respectively.

$$\theta_T = -\theta_C \ \{11\}$$

$$\theta_T = 180 - abs(\theta_C) \ \{12\}$$

$$\theta_T = 180 - \theta_C \ \{13\}$$

$$\theta_T = 360 - \theta_C \ \{14\}$$

3.2.2. Relative distance behind turbine

As dynamic power fitness calculation takes wind direction into consideration, the relative distance behind rotor also takes wind direction into consideration. Figure 3 shows how the relative distance behind rotor, s, differs to the distance between two turbines, $\overrightarrow{T_a} - \overrightarrow{T_e}$. Equations 9 and 10 show how the relative distance behind rotor can be calculated.

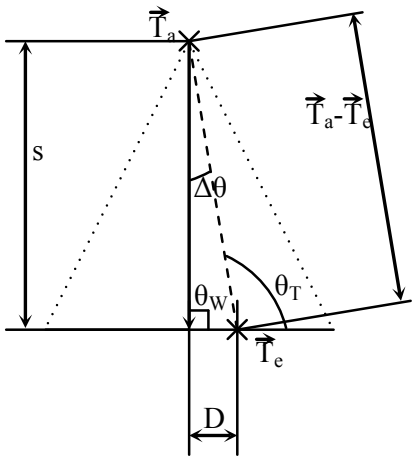

Figure 3 The difference between relative distance behind rotor and true distance between turbines

$$s = \left(\overrightarrow{T_a} - \overrightarrow{T_e}\right) \cdot \cos\left(\Delta\theta\right) \ \{9\}$$

$$\Delta\theta = abs(\theta_W - \theta_T) \ \{10\}$$

In figure 3, the wind direction is the direction where the solid centre line is pointing. The two turbines are marked with crosses, the dotted lines represent the wake cone generated by the turbine in the front (T_a), and the dashed line connects the affecting turbine (T_a) to the affected turbine (T_e). The relative distance behind rotor is marked 's'; the distance between two turbines is marked '$\overrightarrow{T_a} - \overrightarrow{T_e}$', this is the length of the dashed line connecting the two turbines. The angle difference, $\Delta\theta$, in equation 10 is the absolute difference between the wind direction, θ_W, and the angle created by the two turbines, θ_T. The relative distance behind rotor when the wind direction is not aligned with the turbines can be found using equation 9, it uses the true distance between two turbines and the absolute angle difference between the wind angle and turbine angle.

3.2.3. Coverage test

When dealing with unidirectional wind, it is easy to determine if one turbine is affected by the wake of another, by checking if one turbine is behind another, and if the affected turbine is within the wake cone of the front turbine. However, when dealing with dynamic power fitness function, a series of tests needs to be in place to check if one turbine is within the wake cone of another.

The first test is to see if the angle between two turbines is equal to or within the wind angle range. If this is the case, the relative distance behind rotor is equal to the distance between two turbines. If this is not the case, checks need to be implemented to determine if the position of one turbine affects the performance of another.

When the turbine angle is outside of wind angle range, the positivity or negativity of the relative distance behind rotor can be used to determine the relative position of two turbines to each other. An 'if statement' is put in place to check the positivity of the relative distance behind rotor, to determine which turbine is in the front in terms of the wind direction.

Upon the establishment of the relative positions between two turbines, a final check is needed to determine if the affected turbine is within the wake cone of the turbine in front. The distance D labelled in figure 3 represents the shortest distance between the affected wind turbine and the centre of the wake. By checking the distance D and the radius of the wake, the percentage of swept area covered by the wake can be determined. Figure 4 shows 4 scenarios of how distance D relates to the wake diameter, this relationship is important as swept area coverage calculation differs in each scenario.

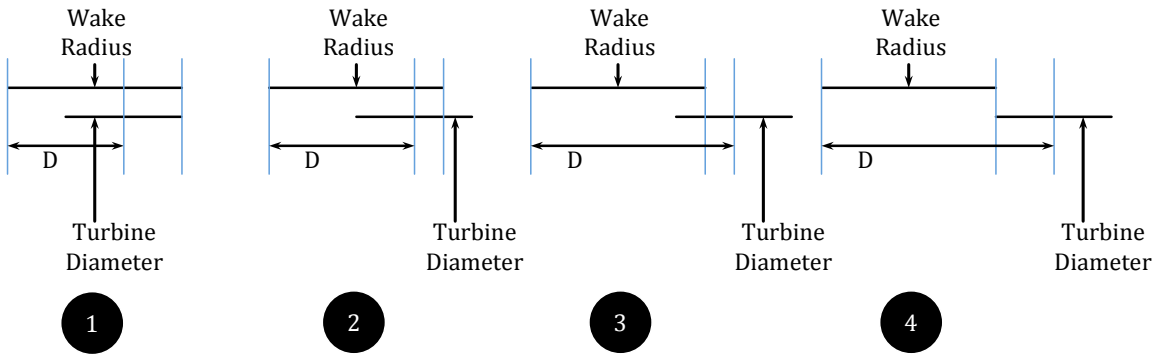

Figure 4 Diagram showing different scenarios of wake cone coverage

In all 4 scenarios shown in figure 4, the top lines represent the wake radius, and the bottom short lines represent the turbine diameter.

The length of turbine diameter covered is used to calculate the percentage of the swept area covered. The percentage of swept area covered is used as a velocity deficit coefficient when the affected turbine is located on the edge of the wake cone. The 4 scenarios shown in figure 4 require different percentage coverage calculations.

The first scenario is completely covered, therefore the coefficient is 1; and the final scenario is completely uncovered, therefore the coefficient is 0.

Scenarios 2 and 3 shows two different types of partial coverage, the first has more than half of the turbine diameter covered, and the second has less than half of the turbine diameter covered. The 2 types of partial coverage can be visualised and is shown in figures 5 and 6 respectively.

The larger circle in figures 5 and 6 represent the wake area; the small circle in figures 5 and 6 represent the turbine area. The yellow shaded regions represent the amount of swept area covered.

The size of the two overlapping areas can be determined using equations 15 to 22. The design and implementation of the overlapping areas (Overlap) are done in 4 parts. The distance between the wake centre and the widest part of the overlapping area, ‘x’, is found using the wake diameter (WD) and the distance between wake centre and turbine centre (D). The width of the overlapping area, ‘a’, is found using the ‘WD’ and ‘x’. The ‘extra’ in equations 17 and 21 denotes the unwanted triangles found when adding the sectors of the two circles. This is taken away when calculating the overlapping areas, which are the chords of the two circles.

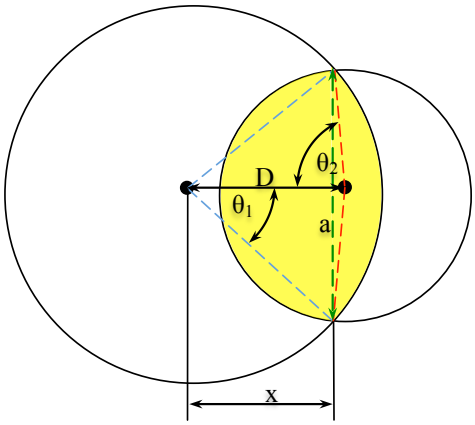

Figure 5 Swept area section covered by wake, in the case when the centre of swept area is covered

$$x = \frac{WD^2 - 1 + 4D^2}{8D} \{15\}$$

$$a = \sqrt{WD^2 - 4x^2} \{16\}$$

$$Extra = \frac{1}{2} aD \{17\}$$

$$Overlap = \frac{\pi}{720} * (180 + \cos^{-1}\left(\frac{2x}{WD}\right) * WD^2 - \cos^{-1}(2x - 2D)) - Extra \{18\}$$

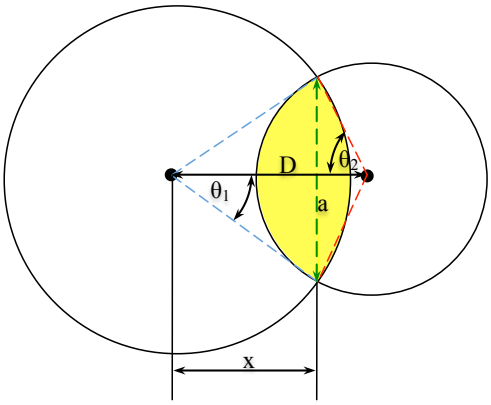

Figure 6 Swept area section covered by wake, in the case when the centre of swept area is not covered

$$x = \frac{WD^2 - 1 + 4D^2}{8D} \{19\}$$

$$a = \sqrt{WD^2 - 4x^2} \{20\}$$

$$Extra = \frac{1}{2} aD \{21\}$$

$$Overlap = \frac{\pi}{720} * (\cos^{-1}\left(\frac{2x}{WD}\right) * WD^2 + \sin^{-1}(a)) - Extra \{22\}$$

3.3. Cost fitness evaluations

The cost is split into capital cost and O&M cost, the costs calculations are shown in equations 4 and 5. Values used in both cost functions are estimates; sources of the estimation are included in the literature review. As the overall aim of the algorithm is to optimise the layout of wind farms, the true numerical values of cost factors are of low priority, in comparison to the ratios between cost factors.

3.3.1. O&M cost

The O&M cost modelled in the fitness function is the sum of the cost to operate onshore office, and the cost to maintain all turbines. The former uses the product of average annual office operation cost and the expected lifespan of the farm; the latter uses the product of average annual turbine maintenance cost, turbine number, and the length of time in which the farm will operate outside of the warranty period.

3.3.2. Capital cost

The capital cost modelled is the sum of basic cost, turbine cost, substation cost, and cable cost. The basic cost will remain constant for all samples, this is the cost related to the farm size and location. As farm size and location remain constant in all samples during simulations, the inclusion of this cost does not affect the optimal layout result. The turbine and substation cost are both related to the number of turbines in the farm. The cable cost describes how spreads out the turbines are in the farm; the implementation of the Steiner Tree Algorithm is detailed in sections 3.3.3. The use of Steiner Tree Algorithm is to determine the minimum cable length required, to connect N number of turbines together, where N is the number of turbines each substation is able to cover. The inclusion of more specific cable cost differentiates the capital cost to O&M, as layout affects the capital cost as well as turbine numbers. If two farm samples have the same number of turbines and power output, the sample with N number of turbines grouped more closely would dominate the other in capital cost objective, as this would lower cable cost hence lower the overall capital cost.

3.3.3. Steiner Tree Algorithm

Route inspection algorithm and Steiner Tree Algorithm are compared, to determine the algorithm that suits the purpose of finding the shortest route to connect all turbines. It is found that the Steiner Tree Algorithm is most suitable as it finds a shortest route to connect

all available nodes, as opposed to route inspection algorithm, which finds the shortest path to visit every edge available.

The Steiner Tree Algorithm is employed and adapted in the cost fitness function. Changes to the original algorithm are made, as one substation may not be able to cover all the available turbines in a farm. The algorithm needs to be applied as many times as there are substations required, without connecting any turbine twice.

Figure 7 outlines how the Steiner Tree Algorithm is adapted to suit the needs of fitness function, to determine the minimum cable length. Step 1 locates an unconnected turbine; step 2 stores the turbine location in an array. Step 3 finds the distance from all unconnected turbines to turbines in the storage array; step 4 selects the turbine nearest to existing turbines in the array. Steps 5 and 6 update the storage array by adding location of turbine stored in step 4 and updates cable length by adding the shortest distance found in step 4. Step 1 to 6 is first repeated N times, where N is the substation coverage. This is then repeated M times, where M is the number of substations required. Once all turbines are covered, the cable length is recorded.

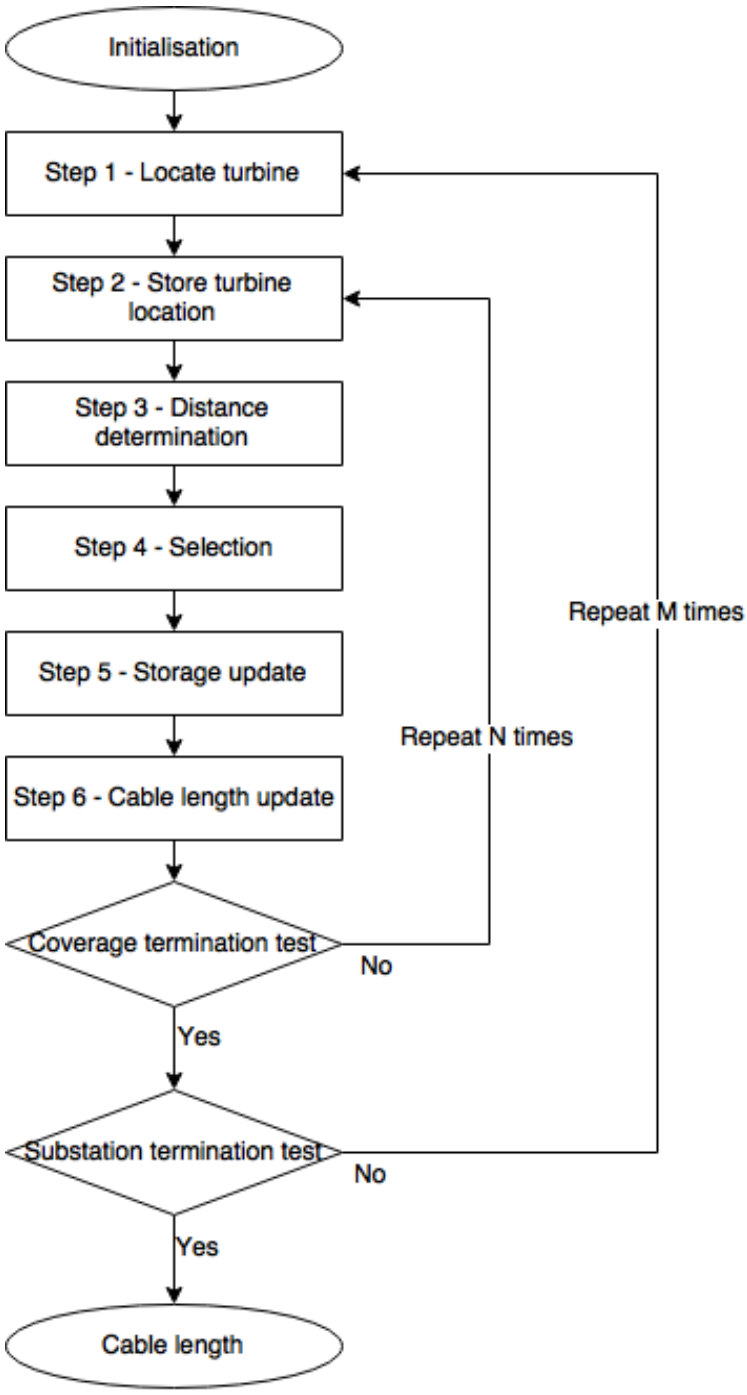

Figure 7 Flow chart describing the adapted Steiner Tree Algorithm

3.4. Multi-objective genetic algorithm design

The MOGA design is based on IVEGA presented by Zhang & Fujimura *(Zhang and Fujimura, 2010)*. Figure 8 shows the evolving process of IVEGA.

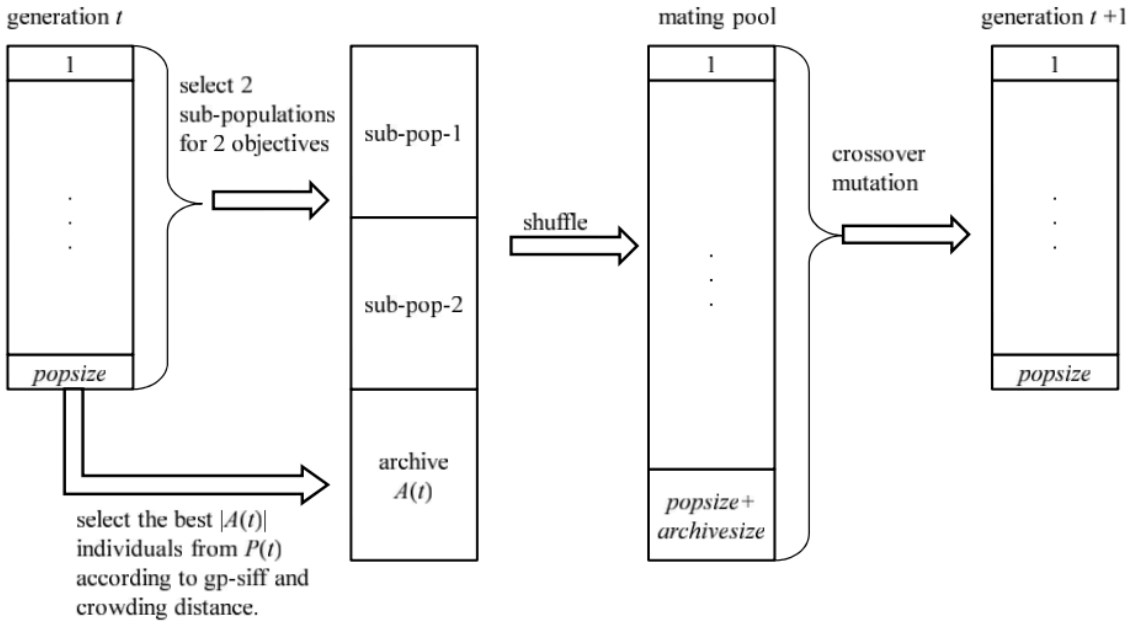

Figure 8 The evolving process in one generation of IVEGA *(Zhang and Fujimura, 2010)*

From figure 8, the fitness of N_P samples at time t are evaluated; the non-dominated solutions from the current samples are added to the archive. The archive is the 'elitist mechanism', which stores all non-dominated solutions. Once the current non-dominated solutions are tentatively archived, all current samples are combined with the tentative elite population in the archive. This is shuffled to form a mating pool, which selects multiple solutions to perform crossover and mutation operations until a new population of size N_P is generated. This process repeats until termination criteria are met, often dictated by the iteration number.

The general method of IVEGA is employed for wind farm layout optimisation. Figure 9 shows the flow chart of the adapted IVEGA algorithm. Figure 8 encapsulates the process of IVEGA between each step; the main differences between IVEGA shown in figure 8 and the adapted version shown in figure 9 are the generation of the mating pool and the selection process. For mating pool generation, rather than shuffle the previous sub-populations and tentative archive, the mating pool used is the combination of the two without any reshuffling. For selection, random seeds are planted in each trial; theses seeds are used to select samples to be operated on and generate a new population set.

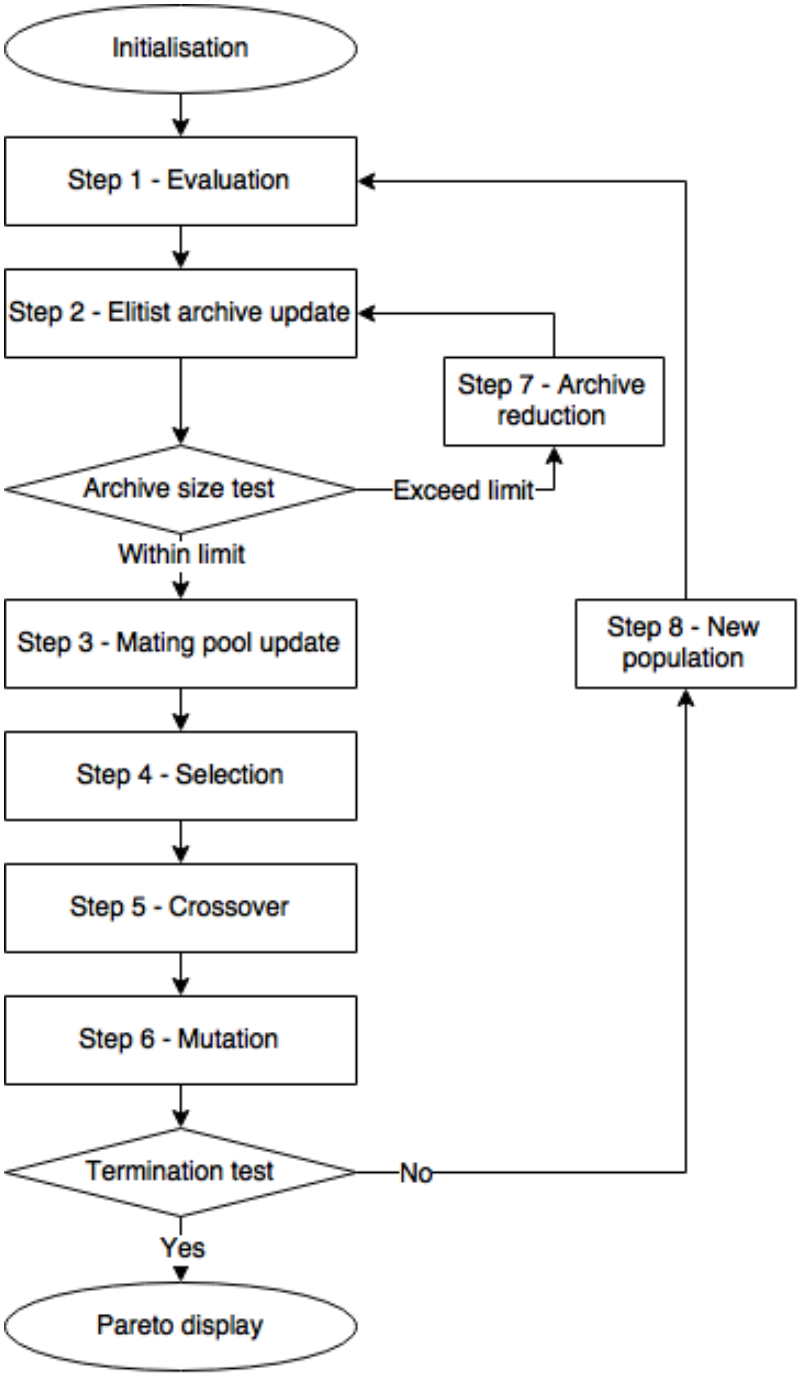

Figure 9 Flow chart of Improved Vector Evaluated GA

3.4.1. Initialisation

The initialisation process generates and rectifies N_P new samples. The generation process randomly places turbines in a given farm, the result is a matrix of '1's and '0's representing the presence or absence of turbines respectively. Obstacles can be added to the generation process, where a given area is valued at zero at the end of the function, thus removing any turbines placed in the region.

By eliminating one turbine in pairs that are too close together, the rectifier function ensures that distances higher than the minimum separation distance separate all turbines.

3.4.2. Crossover and mutation

The crossover and mutation processes are used to generate new populations from a mixing pool. Once two layout samples are selected, the crossover operator generates a random seed to decide whether to perform crossover horizontally or vertically, then, another random seed is generated to decide the point where two selected samples switch.

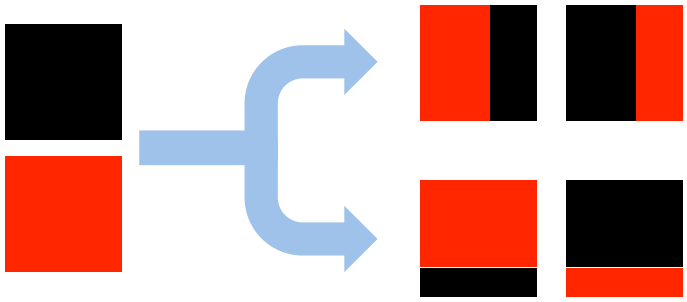

Figure 10 Two types of crossover operation

Figure 10 shows the 2 types of crossover operations. The two squares on the left represent the selected samples. The four squares on the right represent 2 different output sets; the top set shows the samples mixed vertically, the bottom set shows the samples mixed horizontally.

The mutation operator randomly selects a farm location; the value within the location selected is then randomly redefined to '1' or '0'.

3.4.3. Archive reduction

The research on IVEGA by Zhang & Fujimura *(Zhang and Fujimura, 2010)* has used the gp-siff coupled with individual crowding distance to reduce the size of the archive. The archive file stores a pre-defined number of non-dominated solutions, the limit is used to lower the computation cost.

$$eval(S_i) = p(S_i) - q(S_i) + c \quad \{23\}$$

Equation 23 shows the gp-siff value, eval(S_i), is evaluated by Zhang & Fujimura for sample i. It uses the number of other samples dominated by sample i, p(S_i), the number of other samples that have dominated sample i,q(S_i), and the total number of participating samples, c.

Equation 23 includes the number of samples dominated by sample i, as well as the number of samples that dominate sample i. The resultant gp-siff values would be useful to determine several layers of Pareto front. Since the archive used in the algorithm in this project only aims to store the optimal layer of Pareto value, $q(S_i)$ would be 0 for all samples, otherwise the stored sample would have been replaced by another. Equation 24 shows the adapted gp-siff value calculation.

$$eval(S_i) = \frac{p(S_i)}{t} \{24\}$$

As in equation 23, $eval(S_i)$ and $p(S_i)$ in equation 24 represent the gp-siff value of sample i, and number of dominated samples by sample i respectively. To eliminate any advantage early stored samples may have over late stored samples in the archive, the iteration number 't' is added. It represents the number of iterations a particular sample has remained in the archive array. Higher gp-siff value indicates better solutions, as the solutions would have dominated more samples in fewer numbers of iterations.

If several samples have the same gp-siff value, individual crowding distances are then used to differentiate samples. Figure 11 is from research by Deb et al. on NSGA-II *(Deb et al., 2002)*; the figure shows how crowding distances can be found for Pareto front values.

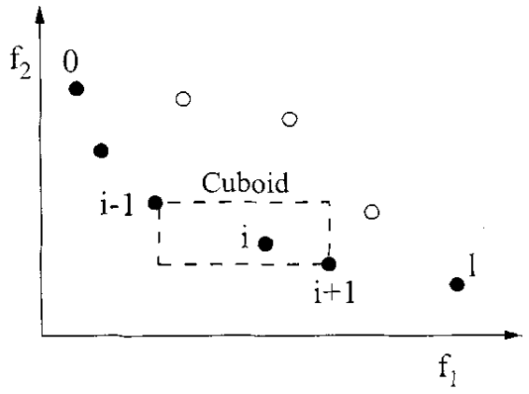

Figure 11 Crowding distance calculation *(Deb et al., 2002)*

In figure 11, the filled in circles are the Pareto front. The crowding distance of a sample, in a bi-objective algorithm, is the area (cuboid) between the previous and following samples of the sample measured. This can be extended to three objective algorithms, where the volume between two nearest samples represents the crowding distance. The use of crowding distance eliminates samples that have fitness values very similar to nearby samples on the Pareto front.

When calculating the crowding distance, the fitness values for each objective needs to be converted to nominal fitness. This is to eliminate any uneven crowding distance contribution by objectives, due to difference objective scales.

$$F_N = \frac{F_T - F_{\min}}{F_{max} - F_{min}} \{25\}$$

Equation 25 shows how the nominal fitness (F_N) is calculated. It uses the true fitness value (F_T), current minimum fitness value (F_{min}) and current maximum fitness value (F_{max}). The application of this equation resizes all objective values to be in the range of 0 and 1.

As the first and final Pareto value only has 1 nearby Pareto value, the crowding distance value is found by the volume between itself and the nearest Pareto value multiplied by 2^N, where N is the number of objectives in the algorithm.

3.5. Algorithm testing

Individual functions are tested separately, with experiments designed to emphasise the purpose of the function, and ensure the functions work as intended.

3.5.1. Power function test

The power function is tested in two parts. The first is to test how the angle and separation distance affects the total power output, by applying multidirectional wind on farms with the same layout in respect to wind direction. The wind directions tested are 0°, 90°, 180° and 270°, the separation distance is tested between 1 and 100 rotor diameters. The change in wind angle is expected to not affect the power output, as long as the farm layout relative to the wind direction remains the same. However, power output is expected to increase with the separation distance, as the increase in separation distance would decrease velocity deficit caused by wake.

The second power function test aims to visualise the summing of wake effect, a unidirectional wind is used on a farm of size 81 rotor diameters squared, with turbine separation distance of 16 rotor diameter. The use of large farm size gives a wide range of velocity distribution to be visualised; and the use of even turbine spread with unidirectional uniform wind makes the expected velocity distribution more predictable.

In order to visualise the velocity distribution across the farm, the function is modified. Instead of calculating wind velocity at each turbine location, the wind velocity is calculated at

every cell across the farm. The complete velocity distribution is expected to show some wake cones overlapping with each other.

3.5.2. Capital cost function test

The capital cost function is tested in three parts. The first is to test the function with minimum cable cost contribution, the test is performed on a farms with turbines in a straight line, with a separation distance of 1 rotor diameter. The total number of turbines in a line is increased throughout the experiment. The cost is expected to display a linear relationship to turbine number, with discreet cost increments at multiples of substation coverage limit.

The second experiment aims to determine if the Steiner Tree Algorithm is implemented correctly. The capital cost function is tested on farms with the same turbine number; where turbines are in a grid layout (4 turbines forming a square shape). With the turbine number remaining constant, the capital cost should increase linearly with the increase of separation distance (from 1 to 20 rotor diameters).

The third experiment aims to determine the effectiveness of the Steiner Tree Algorithm. Using constant farm size and turbine number (4), random layouts are generated. The result is expected to show farms with more closely located turbines to have lower capital cost compared to more spread out turbine layouts.

3.5.3. O&M cost function test

The O&M cost is shown in equation 5, this cost is solely dependent on the total number of turbines in a farm. A simple experiment is planned to show the expected linear relationship between turbine number and O&M cost. This experiment is done by linearly increasing the total number of turbines and determines the total O&M cost.

3.5.4. Archive reduction test

The archive reduction techniques used are gp-siff and crowding distances. To save computation time and to isolate the function effect, a set of archive values are generated and stored separately. This allowed the function to be tested, observed, and improved where necessary, without the complete program simulation each time. The archive values stored will be obtained from a simulation on a small farm size (5 rotor diameters) with low separation distance (2 rotor diameters), and a low number of iterations (50). The parameter combination used would require short simulation time. The chance of Pareto front samples having the

same gp-siff value is high due to low iteration number, therefore allowing both the gp-siff and crowding distance to be observed.

The final archive function is expected to reduce the number archived results. First by the gp-siff values of samples, samples with smallest gp-siff values are to be eliminated first. If two or more samples have the same gp-siff value, the crowding distance is then used to differentiate samples, and sample with the smallest crowding distances are eliminated first. This can be observed by changing the archive size limit, and checking to see if the orders of sample eliminations are as expected after each limit reduction.

3.5.5. Small farm layout analysis

The optimal layout of small farms with low separation distances can be analytically estimated more easily than large farms. A small farm size of 5 rotor diameters squared, with low separation distance of 2 rotor diameters, and 500 iterations will be used as an example, to show that the Pareto front layout results obtained by the algorithm are as expected. The small farm size and separation distance allow easy analytical predictions to be made, the use of high iteration number would ensure the resultant farm layouts are fully optimised. To reduce computation cost, the wind used will be unidirectional (0°) and uniform ($14ms^{-1}$). Several farm layouts from either ends of the Pareto front will be displayed; these are expected to correspond to expected layouts with highest power output, or lowest costs.

3.5.6. Large farm Pareto analysis

Once the algorithm has shown the capability to accurately optimise small farms, the algorithm is then applied to a larger farm with 20 rotor diameters squared, with minimum separation distance 3 rotor diameters, through 500 iterations. The resultant layouts are expected to be near optimum.

The expected relationship between the two cost factors are near linear, with expected variations due to substation and cable cost, as both cost objectives are predominately dependent on the total turbine number. The relationship between the power output and costs are expected to resemble an exponential curve; where the first few turbine additions in a near empty farm have a large percentage impact on the total power, and when the farm is nearly filled, any additional turbines have very little or no effect on the power output.

4. Presentation of experimental result

4.1. Power function

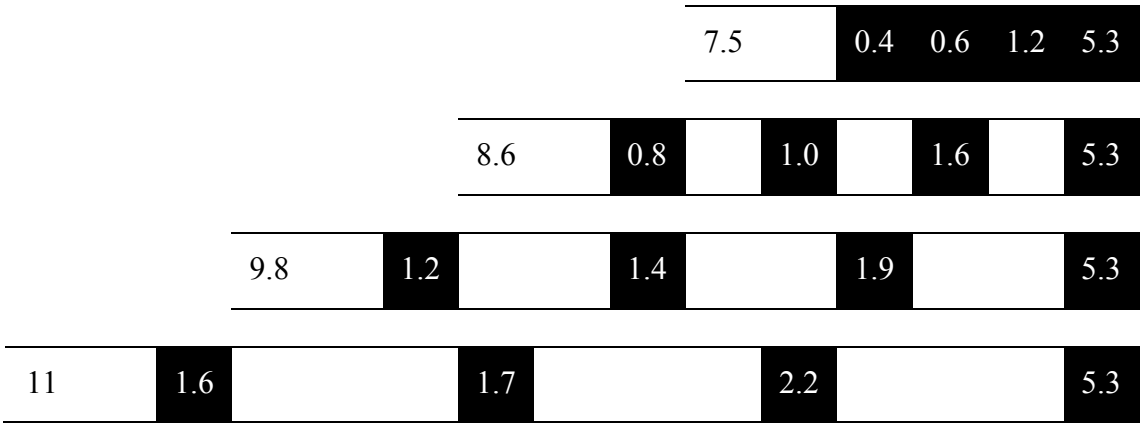

Figure 12 Four farm layouts showing power increase as separation distance increase

Figure 12 shows 4 separate farm layouts, the filled in squares represent the presence of wind turbines. The four farms shown above have separation distances of 1, 2, 3 and 4 rotor diameters respectively. The wind direction used is 0° and the wind velocity is 14ms^{-1}. The numbers at turbine locations are the turbine power output in mega watts and the numbers at the far left of each farm represent the farm power output in mega watts.

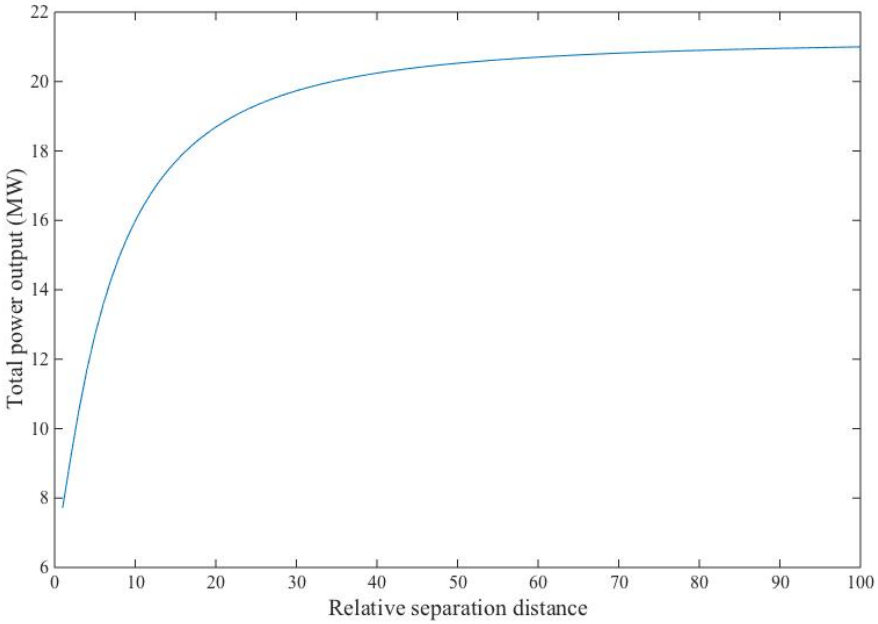

Figure 13 Relationship between total power output of 4 turbines and the relative separation distance between each turbine

Figure 13 shows the relationship between separation distance and farm power output, the farm layout used is the same as layouts shown in figure 12, the separation distance is increased whilst its effect on power output is measured. The separation distance and farm power output have an inverse exponential relationship, as shown in figure 13.

The four farms shown in figure 12 are rotated by 90°, 180° and 270°, the wind direction in each rotated scenario is also rotated by the same angle. The results have shown that farms with the same layout relative to the wind direction have the same power output, indicating successful implementation of the dynamic power function.

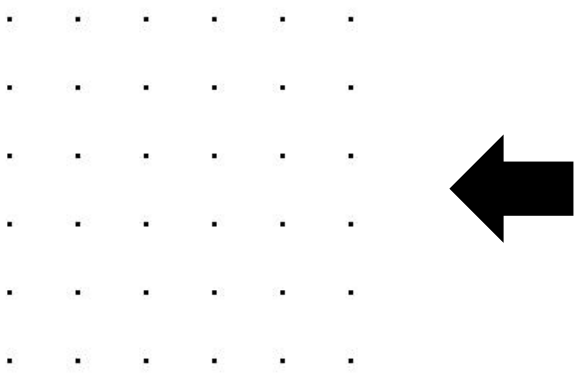

Figure 14 A square grid layout with wind coming in at 0 degrees, black dots represent turbine positions

Figure 14 shows a wind farm layout of farm with 81 rotor diameters squared. There are 36 turbines spread evenly, with 16 rotor diameters between each turbine and its nearest neighbour. Figure 15 shows the resultant velocity distribution of the farm shown in figure 14, with a wind angle of 0° and velocity of 14ms^{-1}. The greyscale represents high and low wind speeds with darker regions representing lower wind velocities. Locations directly in front of the darkest spots are where the wind turbines are located.

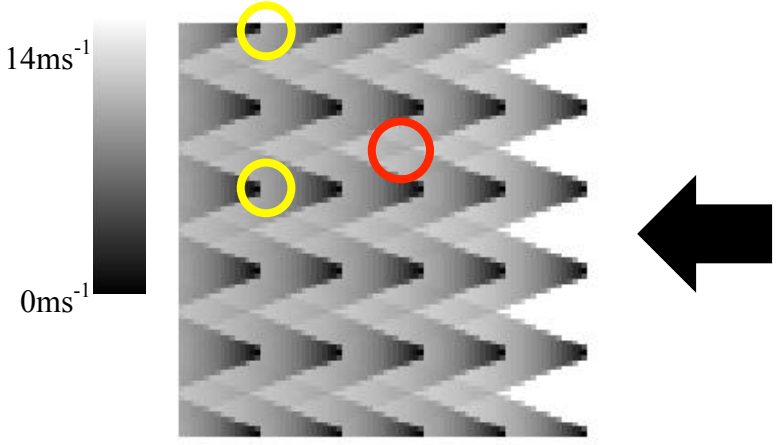

Figure 15 Wind velocity distribution on wind farm with square gird layout

The red circle in figure 15 captures 2 wake-cones overlapping, showing that the velocity is lower at locations where wake cones overlap. The yellow circles captures two turbines in the same vertical column, with one being on the edge of the farm and the other near the centre. The turbine at the farm edge have a power output of 3.87MW compared to the other with a power output of 3.84MW, the difference is due to the two turbines being in a different numbers of wake cones. As the turbine near the centre is affected by nearly twice as many turbine wakes as the turbine on the edge; the power difference between the two turbines shows the wake summing effect numerically.

4.2. Capital cost function

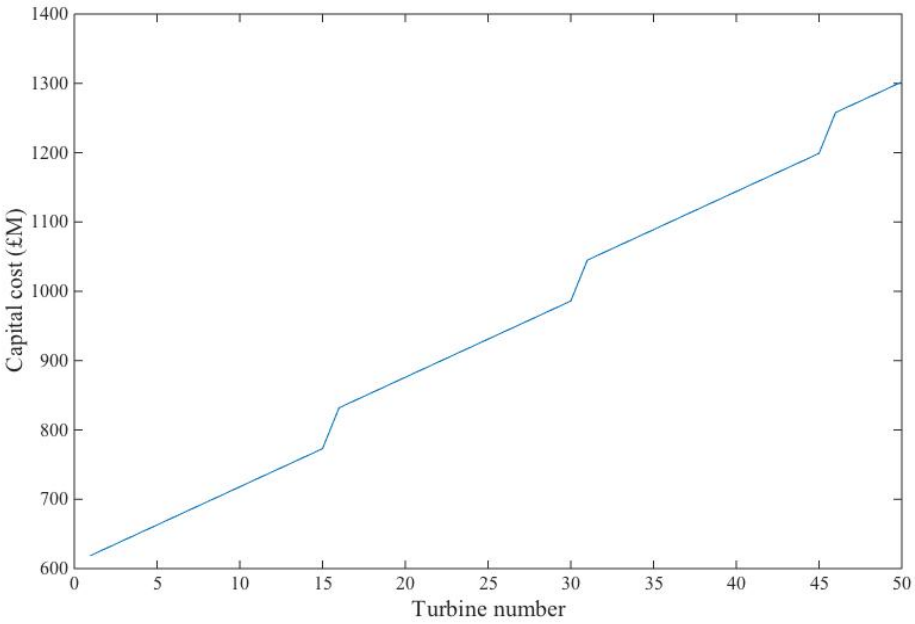

Figure 16 Relationship between turbine number and capital cost

Figure 16 shows the relationship between the total turbine number and capital cost, the substation coverage used is 15 turbines. The cable cost contribution is minimised by arranging the turbines in a straight line. The resultant near linear relationship between turbine number and capital cost is as expected, with discrete capital cost increments every 15 turbines.

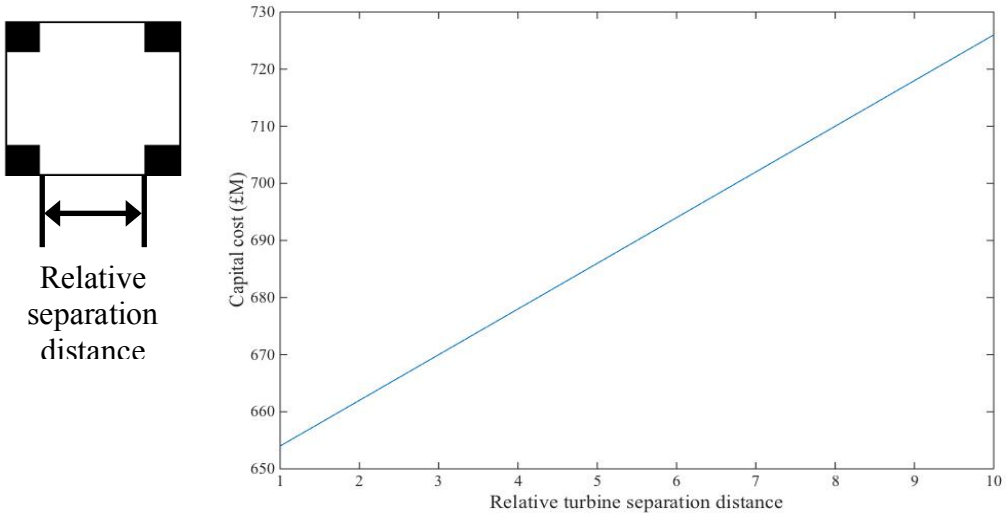

Figure 17 Simple farm layouts with 4 turbines on corners, showing the relationship between separation distance and capital cost

Figure 17 shows how the separation distance affects the cable length and cost. The left image in figure 17 shows how 4 turbines are located relative to each other; the relative separation distance between turbines are increased from 1 and 10. The constant turbine number eliminates all other cost factors in in the capital cost and focuses the result on the cable cost. The results have shown a linear relationship between the turbine separation distance and capital cost. The linear relationship is expected due to the basic nature of the layout; it is evident that the shortest distance to connect all 4 turbines will increase linear with separation distance.

£676.8M £665.5M £656.9M £670M £662M

Figure 18 Random farm layouts with a limited turbine number, showing effects of cable cost

Random farm layouts are shown in figure 18, the 5 layouts have the same farm size and turbine number (4, in white), the capital cost of each layout is listed below the layout. The variation in capital cost between farms in figure 18 is evidence of successful implementation

of Steiner Tree Algorithm. As farm capital cost is lower for farms with turbines more closely grouped together.

4.3. O&M cost function

Figure 19 shows the linear relationship between turbine number and O&M cost, the linear result is as predicted as the model used for O&M cost calculation show that the O&M cost is solely dependent upon the total number of turbines.

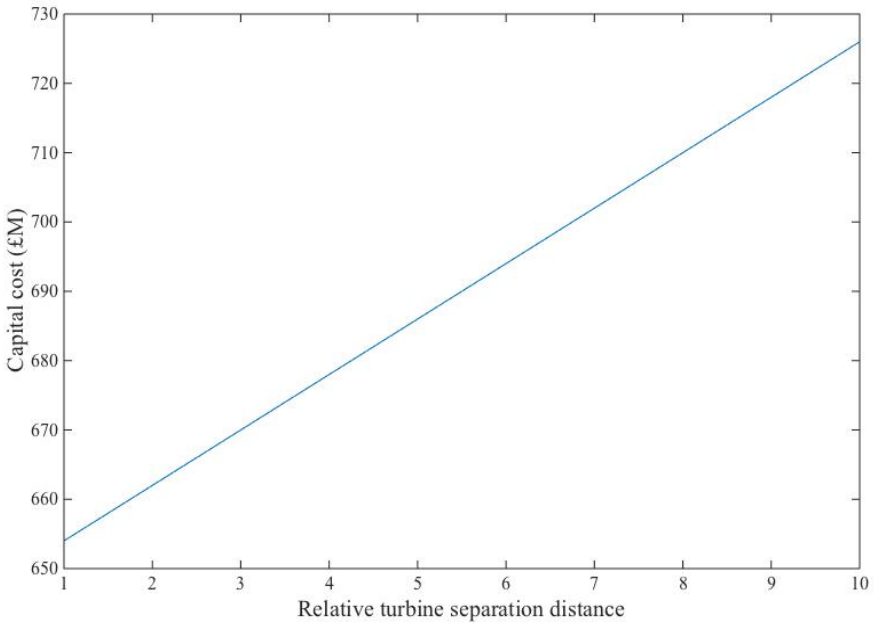

Figure 19 Relationship between the turbine number and O&M cost

4.4. Archive reduction techniques

Table 1 Objective fitness and domination number of small farm sample

No.	True power fitness	Nominal power fitness	True capital fitness	Nominal capital fitness	True O&M fitness	Nominal O&M fitness	Number of dominations	Trial number
1	18.4	0.96	674	0.60	39.0	0.63	63	23
2	18.6	0.97	689	0.76	40.5	0.75	56	38
3	18.5	0.96	685	0.72	40.5	0.75	104	45
4	18.9	0.99	700	0.88	42.0	0.88	73	48
5	18.7	0.98	698	0.86	42.0	0.88	123	50
6	19.0	1	711	1	43.5	1	269	50

7	9.9	0.27	641	0.24	34.5	0.25	1	51
8	5.3	0	619	0	31.5	0	0	51
9	14.0	0.64	652	0.37	36.0	0.38	11	51
10	7.8	0.18	630	0.13	33.0	0.13	0	51
11	14.7	0.69	665	0.50	37.5	0.50	13	51

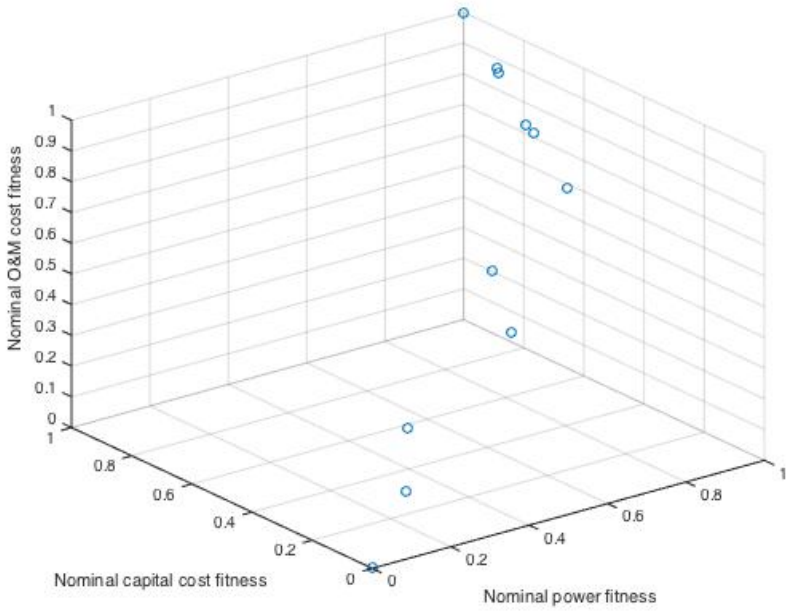

Figure 20 Nominal fitness of optimised layout in small farms, through low number of iterations

Table 1 shows the true objective fitness, nominal objective fitness, number of dominations the iteration number of 11 optimised samples. As shown in equation 24, gp-siff values can be calculated using the number of dominations and trial number. Samples are eliminated in the order of gp-siff values, with the smallest gp-siff value eliminated first. When the gp-siff values of two samples are the same, the crowding distance of the two samples are then compared. Samples with smaller crowding distances are eliminated first, as higher crowding distance means the sample have more unique attributes.

When the archive size is steadily reduced, with one sample eliminated at the time. The order of elimination is as expected. Sample number 10 is eliminated first, although it has the same gp-siff value as sample 8, sample 10's crowing distance is smaller than that of sample 8, therefore it is eliminated first. After the elimination of sample 10, all other samples left in archive have different gp-siff values; thus all are eliminated by the order of the gp-siff value

from smallest first. The correct elimination order proves that the archive reduction methods are implemented correctly.

4.5. Small farm layout analysis

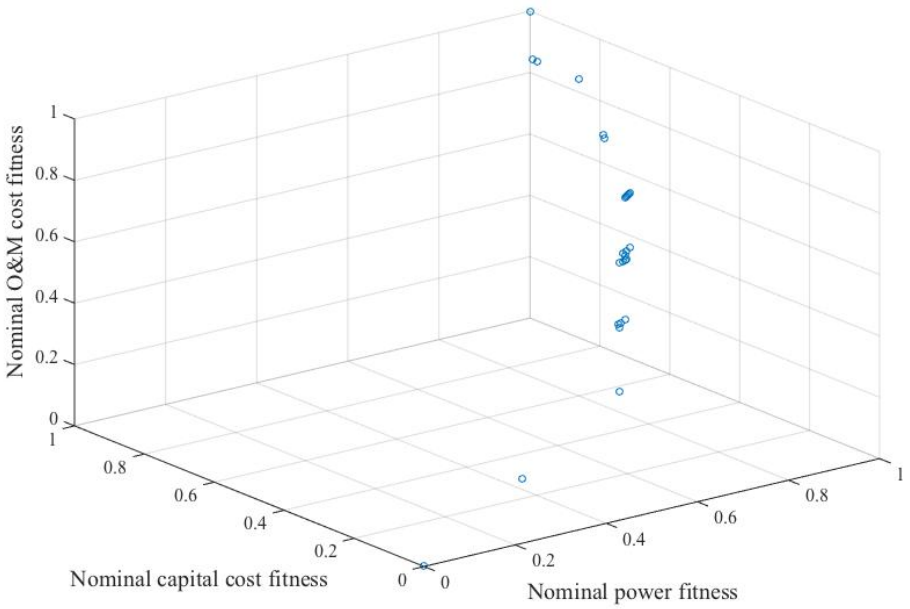

Figure 21 Nominal fitness of optimised layout in small farms, through high number of iterations

Figure 21 shows a Pareto front of a simulation, where each dot represents an optimised farm layout, with corresponding nominal fitness. The farm optimised has size of 5 rotor diameters squared, with a turbine separation distance of 2 rotor diameters. The optimised result is obtained through 500 iterations, with unidirectional (0°) uniform ($14ms^{-1}$) wind to lower computation cost and provide more predictable optimal layout for analysis.

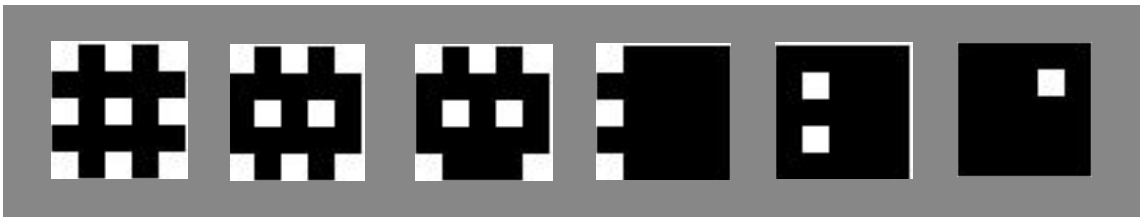

Figure 22 Turbine layouts with high power output (first 3), and low power output and cost (final 3)

Figure 22 shows the exact layouts of several farms on either extremes of the Pareto front. As expected, farms with better power production have higher turbine number and high cost. The first 3 layouts in figure 22 show the turbines layouts of high power farms, the layouts of these farms are evenly spaced out and nearly fills the entire farm, the powers output of the three

high power layouts are 2.277MW, 2.223MW and 2.218MW respectively. In comparison, farms with low costs have low power output, the turbines are laid out so none or very few turbines are under the wake influence of others. The last 3 farm layouts in figure 22 have power outputs of 1.591MW, 1.060MW and 0.530MW respectively. The linear relationship between power and turbine number in the three farms with lowest power output is evidence that there are no wake interactions in these layouts. The farm layout on the extremes of the Pareto front show that the optimised layout for small farms are as expected, and the relationship between cost and power can be analysed for larger farm using Pareto front result.

4.6. Large farm Pareto analysis

Table 2 Nominal fitness of optimised layout in large farms, through high number of iterations

Solution no.	Nominal power fitness	Nominal capital cost fitness	Nominal O&M cost fitness
1	0.9362	0.8660	1
2	1	1	0.8333
3	0.6812	0.4962	0.5
4	0.1164	0.0333	0
5	0.4612	0.2403	0.1667
6	0.8355	0.5396	0.6667
7	0.6834	0.5195	0.5
8	0.9817	0.9339	0.8333
9	0.6681	0.2641	0.3333
10	0.8010	0.5753	0.5
11	0.7417	0.5490	0.5
12	0.4297	0.1466	0.3333
13	0.9277	0.5824	0.6667
14	0.3247	0.0697	0.1667
15	0.3573	0.1169	0.1667
16	0	0	0
17	0.0379	0.0315	0.1667
18	0.2260	0.0478	0

19	0.6790	0.4908	0.5
20	0.9640	0.9135	1

Table 2 shows the nominal fitness of a simulation, each solution number corresponds to an optimised layout. The farm optimised is 20 rotor diameters squared, with a turbine separation distance of 3 rotor diameters. The optimised result is obtained through 200 iterations, with unidirectional (0°) uniform (14ms^{-1}) wind to lower computation cost.

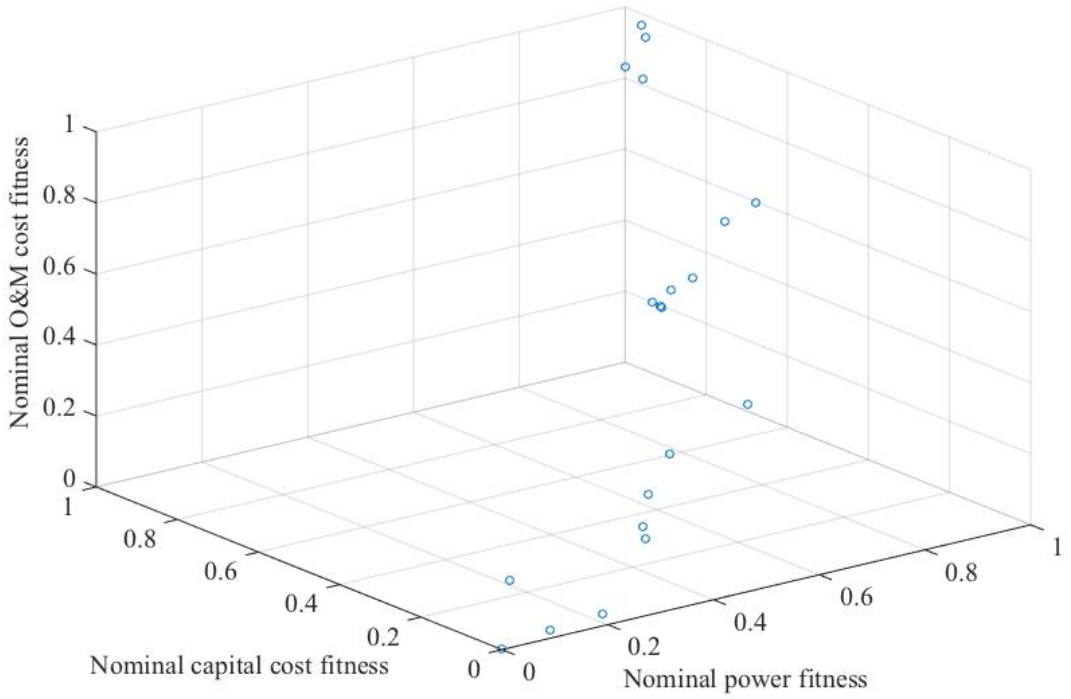

Figure 23 Nominal fitness of optimised layout in large farms, through 200 iterations

Figure 23 shows a 3D scatter plot of the nominal fitness result, showing in table 2. As the 3D scatter plot is difficult to analyse without a curser to rotate the plot; 3 2D scatter plots are presented in figures 24 to 26, separating figure 23 to allow easy analysis.

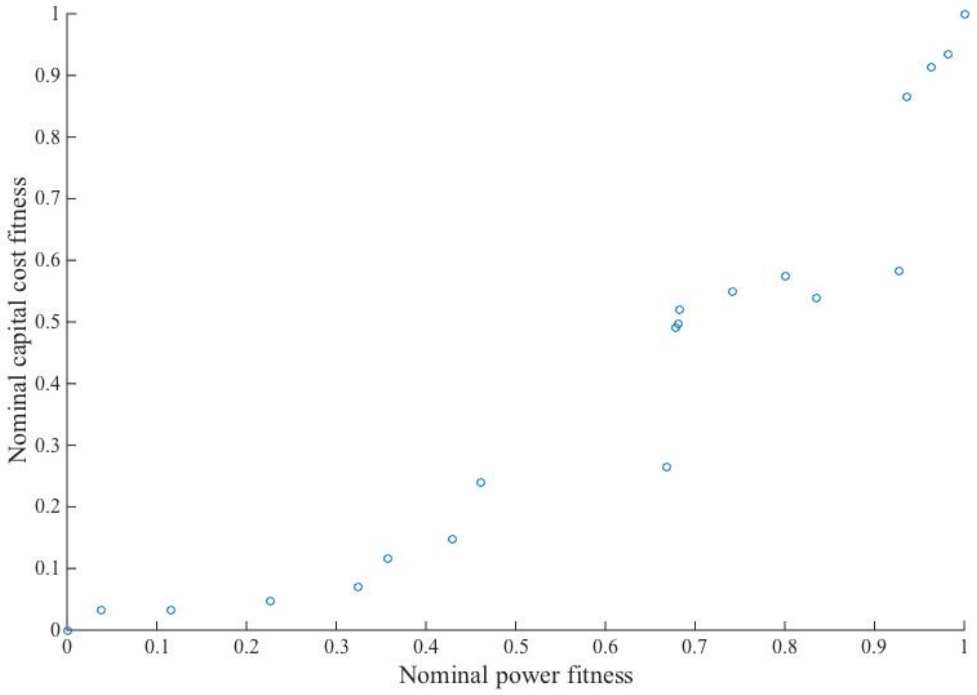

Figure 24 Nominal power and capital cost fitness of optimised layout in large farms, through 200 iterations

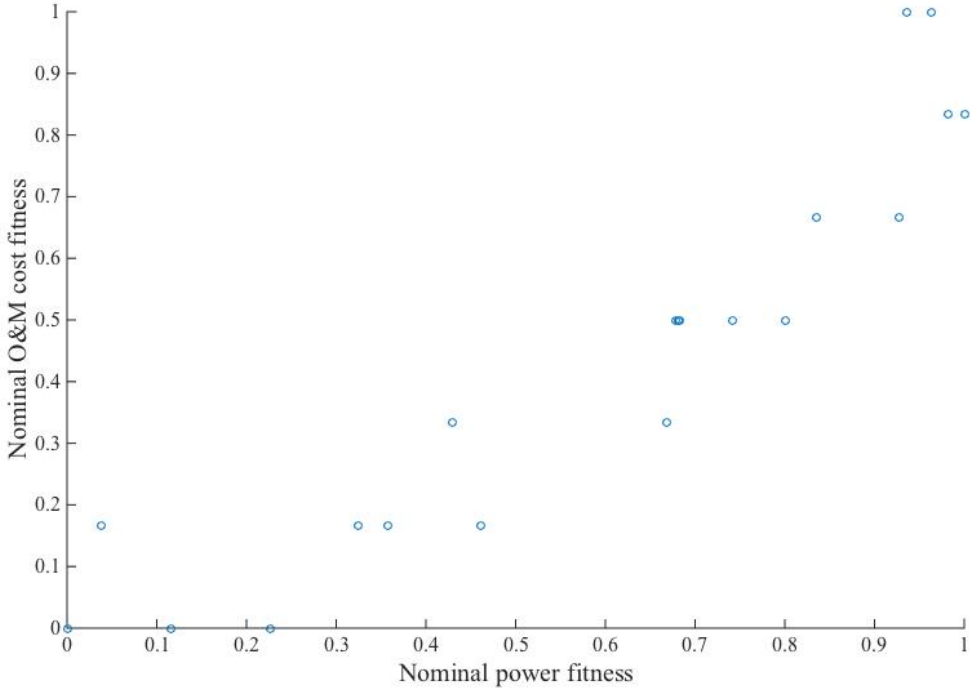

Figure 25 Nominal power and O&M cost fitness of optimised layout in large farms, through 200 iterations

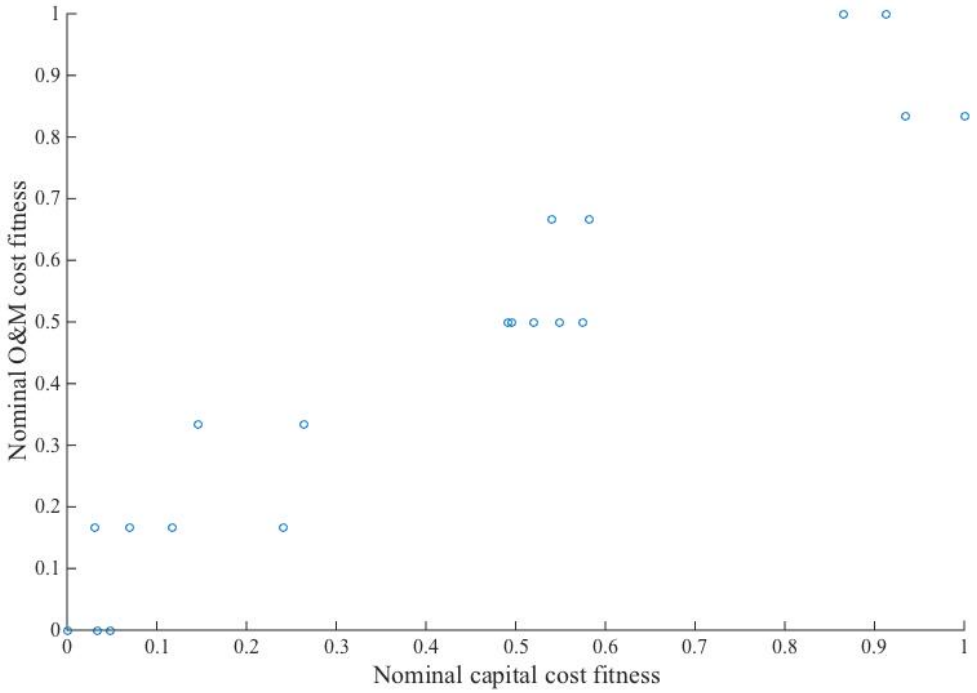

Figure 26 Nominal capital and O&M cost fitness of optimised layout in large farms, through 200 iterations

Figures 24 and 25 show the relationship between power output and two cost factors, capital cost then O&M cost. Both costs have shown a similar relationship to the farm power production, where the initial increase in spending would drastically increase power, however the rate of increase gradually slows, as the farm becomes more populated.

Figure 26 shows the relationship between the two cost factors, this near linear relationship is due to the fact that the turbine number heavily affects both costs. The deviations are cause by the cable cost and substation cost, as discussed after figures 16 and 19.

5. Discussion and conclusions

5.1. Conclusion

Individual function testing has shown all parameters within the functions perform as expected. Some function parameters such as the angle change have being ignored when testing the overall GA, to preserve computation cost. This would not affect the quality of the algorithm, only the current result, as parameters ignored have all shown to work as expected when tested separately.

Results in figure 23 to 26 show the relationship between power and costs of optimal farms, where the power and costs are proportional to each other, but the rate of increase in power slows as the cost increases.

The experimental results have shown that the MOGA has been designed and implemented successfully.

5.2. Further work

To further analyse and utilise the algorithm, greater computational resources and time are needed, to fully incorporate the dynamic angle change and velocity change in the full algorithm simulation.

The current power calculation uses the relationship between power and fluid velocity, with the inclusion wind turbine power coefficient. If detailed power and velocity relations of turbines used are known, the current power function can be modified, to improve the accuracy of power evaluation.

Detailed power calculation also means further collaboration can be done with the team member who have worked on control systems. The inclusion of control systems would require the product of the members' findings, as team members have completed work packages in parallel, the collaboration has not yet been done, but it has been discussed.

The two cost models can both be improved, particularly the O&M model, the current model used is a simplified one, and it solely depends on the number of turbines in a farm. To improve the accuracy of the simulation, more detailed statistical models can replace the current model. One of the reasons such model is not currently available, is because no modern wind farms in the UK have come to the end of their lifetime.

The suggested further work above would make the optimal layout findings better representatives of real world turbine farm, therefore better predicting the cost and power production. All further work suggested above would increase the computation cost.

The main reasons that functions are tested separately, with majority of experiments using small farms and low iteration number, is to lower computation cost and to more closely monitor the effects of individual functions.

6. Project management, consideration of sustainability and health and safety

6.1. Project management

The large project group is formed of nine members, to research and develop techniques to accurately predict the performance of wind farms. Individual members had work packages, which belong to either evaluation or development section.

To effectively monitor and manage group progress, weekly meetings are organised and attended by all members, the project supervisor Gavin Tabor, and postdoctoral researcher Steven Daniels. The roles of chair and secretary of the meetings are rotated weekly amongst members; the roles have the responsibility to produce meeting agenda and minutes. The meetings were an effective way to monitor progress and ensure the group milestones are met.

Various online platforms are used to allow easy file sharing and meeting arrangements. Google Drive is used for file sharing; minutes, agenda and useful papers found by members are all uploaded into separate files on the drive. Facebook is employed as an efficient communication tool, where additional meetings between members are organised to allow effective collaboration, the accessibility of Facebook allowed members to be reached and meetings to be arranged quickly. Lastly, Google Doc and Word Online are used when completing group work, the use of online document eliminates repeated work or any confusion caused by multiple copies of the same work.

The initial aim of this project was to conduct a series of experiments, to use as real data comparison to work done by small scale CFD group; but after several aerofoil experiments, the limitation due to the lack equipment available was realised and a different project direction was considered. The new and revised aim was to develop MOGA to optimise wind farm layout between three objectives.

The Gantt chart presented in figure 27 shows how the project is managed, after the new aim is formulated. Work packages on the new Gantt chart are mostly completed on time, with the exception of the two week SAAB election period. Although several work packages are delayed, running separate function tests have minimised the computation cost, reduced the total time for experimentation and result collection, which effectively mitigated the delay.

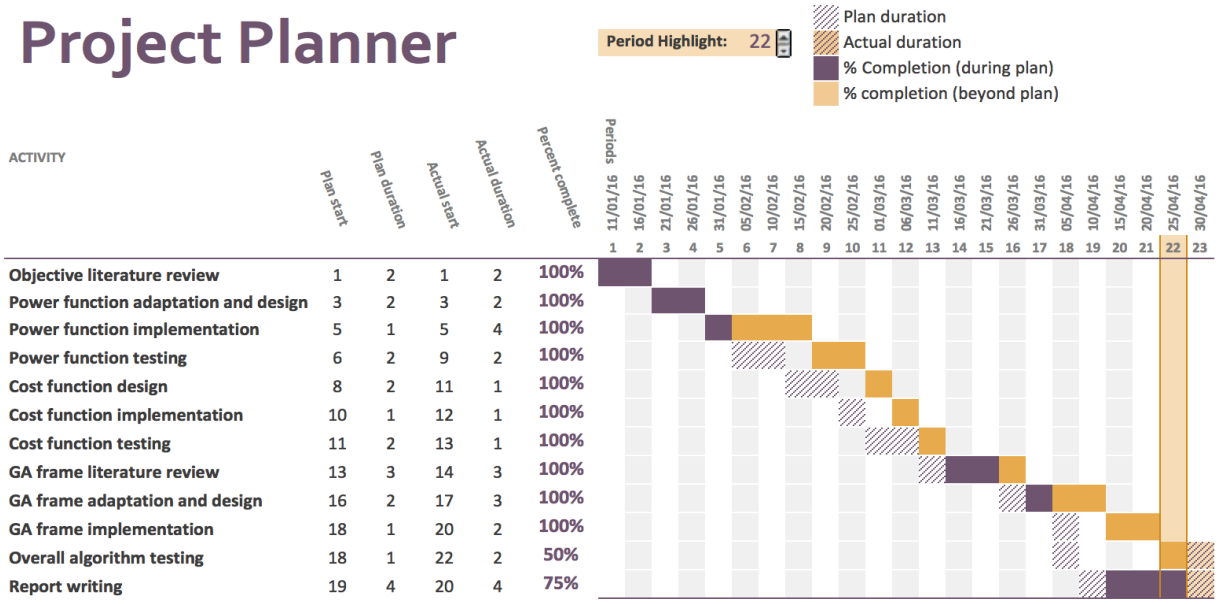

Figure 27 Gantt chart

6.2. Project sustainability

The project sustainability refers to the effective use of resources to minimise the socio-economical and environmental impact of the overall project.

The experimental work done for the initial aim was completed with in house equipment, such as the wind tunnel and 3D printer available in the university; the GA research and development was done on MATLAB. The group budget of £800 was unused by any member of the group.

Throughout the experimental work stage, the wind tunnel and light were switched off when it is not in use; any product designed and printed with the 3D printer are checked several times to minimise the need to reprint. And throughout the development of GA, detailed design work are done on paper, and testing were designed to minimise computation time. Efforts are made towards reducing the total energy consumption, including both equipment and computation usage.

6.3. Health & safety

Health and safety risks are investigated for all aspects of the project; the result of the risk assessment is concluded in table 3. All risk items are rated in terms of importance, which is the product of likelihood and severity; each risk is also discussed qualitatively in terms of cause, effect and action, to mitigate or eliminate all foreseeable risk factors.

Table 3 Risk assessment

Risk item	Likelihood (out of 4)	Severity (out of 4)	Importance (out of 16)	Cause	Effect	Action to minimise risk
Wind Tunnel	2	4	8	Lack of precaution.	Risk of trapped fingers/hair/clothing from fan in wind tunnel.	Take extra care when operating the wind tunnel, especially with hair and tie, make sure all loose objects are either put away or tied up.
Cables and wires	2	2	4	Inefficient equipment keeping around lab.	Trips and falls.	Make sure all plugs are tied to the floor, and tidy away anything that is not being used.
Lab equipment	4	2	8	Lack of monitoring, carelessness.	Equipment overheating, damage.	Test components before use. Make sure components do not operate beyond operation limits.
Prototype issue	2	2	4	Bad design of prototypes or misuse of wind tunnel conditions.	Prototype fails and data cannot be collected, delay overall project.	Thorough study of prototype design to ensure feasibility. Make a plan B in case prototypes delays project.
Stress and illness	3	2	6	Poor planning of work load, loss of work.	Illness, poor decision making, poor quality of work, project delay.	Make clear plans on how project work will be managed along side other deadlines. Make sure to take regular break and not over work.
Corruption of data	2	3	6	Computer issue, virus.	Loss of work and result.	Regularly store data and result in external or online source.
Display equipment	2	1	2	Improper screen setup.	Eye and back strain.	Appropriate screen and monitor set up before use.

7. Contribution to group functioning

Collaborative works are done with other members in the group. Dynamic implementations of objective functions, such as power and cost models are evaluated and developed by other members in the group. These objective functions are used to calculate farm layout fitness in three different objectives.

From collaboration with Ben Withams, who has evaluated many wake modelling and wake summing methods, he advised the used of the Jenson-Kasik wake model coupled with the square summing method. The model and summing method combination has low computation cost, and can obtain results of acceptable quality. The result of dynamically implemented function are compared to that of the Excel model produced by Withams, the comparison between the wake spread shown in figure 15 matches to that produced by the Excel model.

James O'Leary developed the cost models, but as this project is completed in parallel with project by O'Leary. Only the source materials regarding the cost are compared, the resultant model developed by O'Leary was no implemented, a simpler model was implemented in the MOGA. Further collaborations are done with O'Leary when the algorithm was completed, several low cost layouts are proposed by O'Leary, the power output of these layouts are analysed using the objective function implemented within the MOGA, the cost of each individual layouts are analysed by O'Leary, using detailed cost models developed.

Potential further collaborative work is also discussed with Louis Hudson, who has worked on the turbine control system. The result obtained from Hudson could further improve the accuracy of the power fitness function, where the rate of turbine yaw angle change and more detailed power velocity relationship can both be implemented into the power objective function.

References

Aweo.org. (2016). *Technical Specs of Common Wind Turbine Models [AWEO.org]*. [online] Available at: http://www.aweo.org/windmodels.html [Accessed 12 Oct. 2015].

Deb, K., Pratap, A., Agarwal, S. and Meyarivan, T. (2002). A fast and elitist multiobjective genetic algorithm: NSGA-II. *IEEE Transactions on Evolutionary Computation*, [online] 6(2), pp.182-197. Available at: http://sci2s.ugr.es/sites/default/files/files/Teaching/OtherPostGraduateCourses/MasterEstructuras/bibliografia/Deb_NSGAII.pdf [Accessed 16 Feb. 2016].

GWEC, (2016). *GLOBAL WIND STATISTICS 2015*. [online] Brussels, Belgium: GLOBAL WIND ENERGY COUNCIL. Available at: http://www.gwec.net/wp-content/uploads/vip/GWEC-PRstats-2015_LR_corrected.pdf [Accessed 8 Apr. 2016].

International Renewable Energy Agency, (2012). *RENEWABLE ENERGY TECHNOLOGIES: COST ANALYSIS SERIES*. IRENA Working Paper. [online] Bonn, Germany: IRENA Innovation and Technology Centre. Available at: https://www.irena.org/documentdownloads/publications/re_technologies_cost_analysis-wind_power.pdf [Accessed 22 Feb. 2016].

Ituarte-Villarreal, C. and Espiritu, J. (2011). WIND TURBINE PLACEMENT IN A WIND FARM USING A VIRAL BASED OPTIMIZATION ALGORITHM. In: *41st International Conference on Computers & Industrial Engineering*. [online] El Paso, USA: The University of Texas at El Paso. Available at: http://www.usc.edu/dept/ise/caie/Checked%20Papers%20[ruhi%2012th%20sept]/word%20format%20papers/REGISTRATION%20PAID%20PAPERS%20FOR%20PROCEEDINGS/pdf/210%206%20WIND%20TURBINE%20PLACEMENT%20IN%20A%20WIND%20FARM%20USING%20A%20VIRAL%20BASED%20OPTIMIZATION.pdf [Accessed 15 Feb. 2016].

Kumar, A., Saxena, R. and Kumar, A. (2014). A Comparative Study of the Various Genetic Approaches to Solve Multi-Objective Optimization Problems. In: *2014 International Conference on Issues and Challenges in Intelligent Computing Techniques*. [online] IEEE. Available at: http://0-ieeexplore.ieee.org.lib.exeter.ac.uk/stamp/stamp.jsp?tp=&arnumber=6781261&tag=1 [Accessed 18 Feb. 2016].

Kusiak, A. and Song, Z. (2009). *Design of wind farm layout for maximum wind energy capture*. [online] Available at: http://citeseerx.ist.psu.edu/viewdoc/download?doi=10.1.1.156.2024&rep=rep1&type=pdf [Accessed 12 Feb. 2016].

Mendick, R. (2012). Wind farm turbines wear sooner than expected, says study. *The Telegraph*. [online] Available at: http://www.telegraph.co.uk/news/earth/energy/windpower/9770837/Wind-farm-turbines-wear-sooner-than-expected-says-study.html [Accessed 18 Mar. 2016].

Milborrow, D. (2010). Breaking down the cost of wind turbine maintenance. *Wind Power Monthly*. [online] Available at: http://www.windpowermonthly.com/article/1010136/breaking-down-cost-wind-turbine-maintenance [Accessed 26 Feb. 2016].

Murata, T. and Ishibuchi, H. (1995). MOGA: multi-objective genetic algorithms. In: *IEEE International Conference on Evolutionary Computation, 1995*. [online] Perth, WA, Australia: IEEE. Available at: http://0-ieeexplore.ieee.org.lib.exeter.ac.uk/stamp/stamp.jsp?tp=&arnumber=489161 [Accessed 19 Feb. 2016].

NASDAQ.com. (2016). *Commodities: Latest Crude Oil Price & Chart*. [online] Available at: http://www.nasdaq.com/markets/crude-oil.aspx?timeframe=5y [Accessed 5 Apr. 2016].

npower, (2016). *Wind Turbine Power Calculations*. [online] The Royal Academy of Engineering. Available at: http://www.raeng.org.uk/publications/other/23-wind-turbine [Accessed 17 Feb. 2016].

Planningni.gov.uk. (2016). *Draft PPS 18: Renewable Energy | Annex 1 Wind Energy: Spacing of Turbines | Planning Portal*. [online] Available at: http://www.planningni.gov.uk/index/policy/policy_publications/planning_statements/pps18/pps18_annex1/pps18_annex1_wind/pps18_annex1_technology/pps18_annex1_spacing.htm [Accessed 27 Feb. 2016].

Renewables First. (2016). *What is the cost to operate wind turbines ?*. [online] Available at: https://www.renewablesfirst.co.uk/windpower/windpower-learning-centre/how-much-does-a-wind-turbine-cost-to-operate/ [Accessed 23 Feb. 2016].

Renkema, D. (2007). *Validation of wind turbine wake models*. Master of Science. Delft University of Technology.

Tehranipoor, M. (2008). *Steiner Tree Problem*.

The Crown Estate, (n.d.). *A Guide to an Offshore Wind Farm*. [online] The Crown Estate. Available at: http://www.thecrownestate.co.uk/media/5408/ei-a-guide-to-an-offshore-wind-farm.pdf [Accessed 22 Feb. 2016].

Timperley, J. (2015). Will renewables subsidy cuts mean UK misses out on cheaper electricity?. *Business Green*. [online] Available at: http://www.businessgreen.com/bg/feature/2433980/will-renewables-subsidy-cuts-mean-uk-misses-out-on-cheaper-electricity [Accessed 8 Apr. 2016].

Walford, C. (2006). *Wind Turbine Reliability: Understanding and Minimizing Wind Turbine Operation and Maintenance Costs*. SANDIA REPORT. [online] Albuquerque, New Mexico and Livermore, California: Global Energy Concepts, LLC. Available at: http://prod.sandia.gov/techlib/access-control.cgi/2006/061100.pdf [Accessed 8 Mar. 2016].

Wang, F., Liu, D. and Zeng, L. (2009). *Study on Computational Grids in Placement of Wind Turbines Using Genetic Algorithm*. [online] Nanjing, China: Hohai University. Available at: http://0-ieeexplore.ieee.org.lib.exeter.ac.uk/stamp/stamp.jsp?tp=&arnumber=5335776&tag=1 [Accessed 14 Feb. 2016].

Wind turbines' lifespan far shorter than believed, study suggests. (2016). *The Courie*. [online] Available at: https://www.thecourier.co.uk/news/scotland/82974/wind-turbines-lifespan-far-shorter-than-believed-study-suggests/ [Accessed 29 Feb. 2016].

Wind-energy-the-facts.org. (2016). *Operation and maintenance costs of wind generated power*. [online] Available at: http://www.wind-energy-the-facts.org/operation-and-maintenance-costs-of-wind-generated-power.html [Accessed 25 Feb. 2016].

Windmeasurementinternational.com. (2016). *Wind Turbines*. [online] Available at: http://www.windmeasurementinternational.com/wind-turbines/om-turbines.php [Accessed 26 Feb. 2016].

Withams, B. (2016). *Investigating and validating current wake models for use in predicting the power output and optimising the layout of Offshore Wind Farm Arrays*. Masters of Engineering. University of Exeter.

Zhang, W. and Fujimura, S. (2010). Improved Vector Evaluated Genetic Algorithm with Archive for Solving Multiobjective PPS Problem. In: *2010 International Conference on E-Product E-Service and E-Entertainment (ICEEE)*. [online] IEEE. Available at: http://0-ieeexplore.ieee.org.lib.exeter.ac.uk/stamp/stamp.jsp?tp=&arnumber=5660926&tag=1 [Accessed 20 Feb. 2016].